# Isotope Labeling of Carbon Nanotubes and Formation of $^{12}C-^{13}C$ Nanotube Junctions

Liang Liu and Shoushan Fan*

*Department of Physics and Tsinghua-Foxconn Nanotechnology Laboratory*
*Tsinghua University, Beijing, 100084, China*

*Received July 30, 2001*

The physical properties of carbon nanotubes depend sensitively on their atomic structures including diameter and chirality,[1−3] an intriguing characteristic of nanotubes that has captured the attention of researchers worldwide. Aimed at elucidating this unique property and exploring its applications, various nanotube-based devices have been obtained and characterized.[4−9] It is now widely recognized that well-defined properties and device characteristics of nanotubes require the synthesis of homogeneous nanotube materials. An indispensable prerequisite to such control of nanotube structural homogeneity is an in-depth understanding of the nanotube growth mechanism, a topic that has been under extensive investigation since the discovery of the carbon nanotube.[10] Various theoretical models of nanotube growth have been suggested.[11−17] However, direct experimental evidence to support any of the models is scarce. Here we report a $^{13}C$ isotope-labeling method for revealing the growth mechanism of the multiwalled nanotubes (MWNT) made by chemical vapor deposition (CVD). $^{12}C$- and $^{13}C$-ethylene are introduced successively in designed sequences to grow arrays of aligned MWNTs[18] containing intratube $^{12}C-^{13}C$ junctions on porous silicon substrate. The alignment of the nanotubes allowed post-growth microscopy analysis for locating the positions of catalytic particles and identifying the chemical compositions along the length of the nanotubes. The $^{12}C$ and $^{13}C$ isotope portions along the length of the nanotubes can be clearly identified by micro-Raman spectroscopy. This enabled us to establish a relationship between the feeding sequence of $^{13}C_2H_4$ and $^{12}C_2H_4$ and the locations of $^{13}C$ and $^{12}C$ atoms in the nanotubes relative to the catalyst particles and hence to provide a direct experimental picture for the CVD growth of carbon nanotubes.

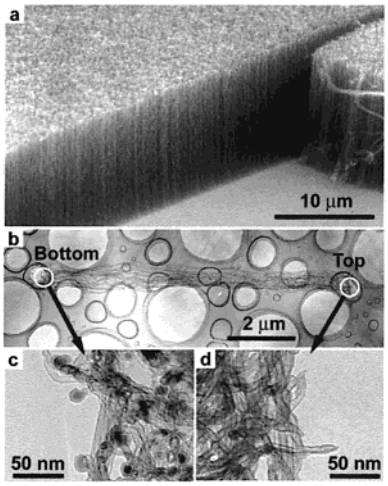


**Figure 1.** Aligned multiwalled carbon nanotubes grown on porous silicon substrates. (a) Scanning electron microscopy picture of an as-grown MWNT array. (b) TEM image of a bundle of nanotubes, the left end is the bottom, the right end is the top. (c) A zoomed-in view of the bottom side of (b), darker particles are catalytic iron particles. (d) A zoomed-in view of the top side of (b), capped nanotube tips are visible.

The porous silicon substrate was prepared by electrochemical etching.[18] A 5 nm thick iron film was electron-beam deposited onto the substrate and then annealed at 300 °C overnight. Nanotube growth was carried out at 700 °C in a 26 mm quartz tube housed in a tube furnace. $^{13}C_2H_4$ or $^{12}C_2H_4$ was flown at 140 sccm (standard cubic centimeter per minute), diluted by a co-flow of 260 sccm of argon under 1 atm pressure for the growth of MWNT arrays. The growth time was 1 min, after which no purification or any other treatment step was taken to the sample. The $^{13}C$-ethylene (both C atoms are $^{13}C$) was obtained from Isotec Co. and had a 99% $^{13}C$ purity. The $^{12}C$-ethylene contained negligible amount of $^{13}C$ isotope at its natural abundance of 1.1 atom %.

The as-grown MWNT arrays had uniform height of 10 $\mu$m, as shown in Figure 1a. For microscopy study, small bundles of MWNTs were pulled out from the array with an atomic force microscope (AFM) tip[19] and carefully transferred onto a transmission electron microscopy (TEM) grid, with their top and bottom ends recognized. TEM (Hitachi H-9000NAR) and X-ray fluorescence (EDX) were used to identify and locate the iron catalyst particles. We found that the iron particles exist only at the bottom ends of the nanotube, while the top ends have abundant capped empty nanotube tips (Figure 1). This shows that the iron particles stayed on the substrate during the growth process due to the strong adhesion between the particles and the porous silicon surface. By tracing individual nanotubes in the bundles under the TEM, we found that the middle parts of the nanotubes were free of breaks and iron catalyst, suggesting that nanotubes grew continuously throughout their length. The nanotubes typically had outer diameters of 10 nm and 6 to 8 inner graphitic shells.

Raman spectra were collected on the sides of the nanotube arrays using a Renishaw micro-Raman spectroscopy equipped with 514 nm laser excitation (incident laser power = 2 mW), the size of the illumination spot is 1 $\mu m^2$. We first grew pure $^{12}C$ and $^{13}C$ nanotube arrays, and recorded their Raman spectra respectively (Figure 2a). The spectra resembled those of typical MWNT materials.[20,21] Importantly, all Raman modes of $^{13}C$ nanotubes ($\omega_{13C}$) exhibited clear shifts to lower frequencies compared to those of $^{12}C$ nanotubes ($\omega_{12C}$), with a uniform ratio

* Correspondence should be addressed to this author. E-mail: fss-dmp@tsinghua.edu.cn.

(1) Saito, R.; Dresselhaus, G.; Dresselhaus, M. S. *Physical Properties of Carbon Nanotubes*; Imperial College Press: London, 1998; Chapter 3.
(2) Odom, T.; Huang, J.; Ki, P.; Lieber, C. M. *Nature* **1998**, *391*, 62.
(3) Wildoer, J. W. G.; Venema, L. C.; Rinzler, A. G.; Smalley, R. E.; Dekker, C. *Nature* **1998**, *391*, 59.
(4) Tans, S. J.; Devoret, M. H.; Dai, H. J.; Thess, A.; Smalley, R. E.; Geerligs, L. J.; Dekker, C. *Nature* **1997**, *386*, 474.
(5) Tans, S. J.; Verschueren, A. R. M.; Dekker, C. *Nature* **1998**, *393*, 49.
(6) Yao, Z.; Postma, H. W. C.; Balents, L.; Dekker, C. *Nature* **1999**, *402*, 273.
(7) Hu, J. T.; Ouyang, M.; Yang, P. D.; Lieber, C. M. *Nature* **1999**, *399*, 48.
(8) Liang, W. J.; Bockrath, M.; Bozovic, D.; Hafner, J. H.; Tinkham, M.; Park, H. *Nature* **2001**, *411*, 665.
(9) Kong, J.; Franklin, N. R.; Zhou, C. W.; Chapline, M. G.; Peng, S.; Cho, K. J.; Dai, H. J. *Science* **2000**, *287*, 622.
(10) Iijima, S. *Nature* **1991**, *354*, 56.
(11) Laurent, C.; Flahaut, E.; Peigney, A.; Rousset, A. *New J. Chem.* **1998**, *22*, 1229.
(12) Kiang, C. H.; Goddard, W. A. *Phys. Rev. Lett.* **1996**, *76*, 2515.
(13) Amelinckx, S.; Bernaerts, D.; Zhang, X. B.; Tendeloo, G.; Landuyt, J. *Science* **1995**, *267*, 1334.
(14) Amelinckx, S.; Zhang, X. B.; Bernaerts, D.; Zhang, X. F.; Ivanov, V.; Nagy, J. B. *Science* **1994**, *265*, 635.
(15) Maiti, A.; Brabec, C. J.; Bernholc, J. *Phys. Rev. B* **1997**, *55*, R6097.
(16) Kanzow, H.; Ding, A. *Phys. Rev. B* **1999**, *60*, 11180.
(17) Sinnott, S. B.; Andrews, R.; Qian, D.; Rao, A. M.; Mao, Z.; Dickey, E. C.; Derbyshire, F. *Chem. Phys. Lett.* **1999**, *315*, 25.
(18) Fan, S. S.; Chapline, M. G.; Franklin, N. R.; Tombler, T. W.; Cassell, A. M.; Dai, H. J. *Science* **1999**, *283*, 512.
(19) Dai, H. J.; Hafner, J. H.; Rinzler, A. G.; Colbert, D. T.; Smalley, R. E. *Nature* **1996**, *384*, 147.

10.1021/ja0167304 CCC: $20.00 
Published on Web 10/26/2001

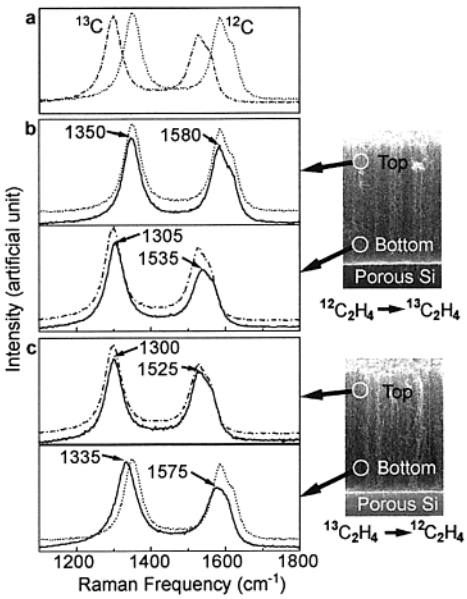


**Figure 2.** Micro-Raman spectra of isotope-labeled MWNT arrays. (a) Pure $^{12}C$ nanotube array (dotted) and pure $^{13}C$ nanotube array (dash−dotted) spectra. (b) Nanotube arrays grown with $^{12}C$ ethylene first and then $^{13}C$ ethylene. (c) Nanotube arrays grown with $^{13}C$ ethylene first and then $^{12}C$ ethylene. The solid curves in the left plots are Raman spectra recorded at the locations circled in the right-hand side images; pure $^{12}C$ or $^{13}C$ spectra are also plotted for comparison (upshifted for clarity).

of $\omega_{13C}:\omega_{12C} \approx 0.96$. Considering that the frequencies of Raman modes are inversely proportional to the square root of the atomic mass, and that the respective forces constants in the $^{12}C$ and $^{13}C$ nanotubes are equal, we readily derive that the frequencies of the Raman modes of $^{12}C$ and $^{13}C$ nanotubes are related by,

$$\omega_{13C} = \omega_{12C} \times \sqrt{m_{12C}/m_{13C}} = \omega_{12C} \times 0.9608$$

this is in excellent agreement with our experimental finding and implies that for nanotubes grown under designed $^{12}C_2H_4$ and $^{13}C_2H_4$ feeding sequences, micro-Raman spectroscopy can readily locate the position of the $^{12}C$ and $^{13}C$ isotopes in the nanotubes.

Two feeding sequences of isotope ethylene were used for the growth of $^{12}C-^{13}C$ nanotube junction arrays. In the first sequence, $^{12}C$ ethylene was introduced for 15 s and then switched to $^{13}C$ ethylene for another 45 s.[22] To avoid any possible disturbance to the growth process, no purge step was taken to deplete $^{12}C$-ethylene before introducing $^{13}C$-ethylene. Micro-Raman measurements revealed that at the top of the nanotubes arrays, the nanotubes consist of purely $^{12}C$, while at the bottom, the nanotubes consist of mostly $^{13}C$ (Figure 2b).[23] Since $^{12}C$ was fed into the system earlier than $^{13}C$, the result clearly reveals that the top segments of the nanotubes are formed chronically earlier in the growth process than the lower segments. Combined with the finding that the catalyst particles reside at the bottom of the nanotube array, this leads to a clear extrusion growth picture of the nanotubes, as schematically shown in Figure 3. The iron

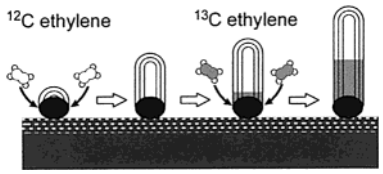


**Figure 3.** Growth model of MWNTs. The black oval is the metal catalyst attached to the substrate (white dotted region), the shaded zone in the nanotube and the ethylene molecular represents the $^{13}C$ isotope atoms. Four snapshots from left to right show the growth process of a $^{12}C-^{13}C$ nanotube junction.

catalyst particle stays on the substrate throughout the growth process. Initially, a $^{12}C$ nanotube segment grows out from the catalyst to a certain length when $^{12}C$ ethylene is introduced into the system. As the gas source is switched to $^{13}C$ ethylene, a $^{13}C$ nanotube stem grows out from the catalyst, pushing the already grown $^{12}C$ segment upward and forming a $^{12}C-^{13}C$ nanotube junction. Thus, the combined microscopy and microspectroscopy studies unambiguously reveal that the extrusion mechanism[14,17] operates in our CVD grown of MWNTs, and rule out any other possible growth mechanisms.

The second feeding sequence was inversed, in that $^{13}C$ ethylene was first introduced for 15 s and then $^{12}C$ ethylene for 45 s. In this case (Figure 2c), the Raman spectra clearly revealed that the $^{13}C$ atoms were at the top segments of the nanotubes and the late introduced $^{12}C$ atoms were at the bottom segments of the nanotubes, which reinforces the nanotube growth mechanism described above.

From the Raman spectroscopy results shown in Figure 2, one clearly sees that the top segments of the nanotubes consist of only the first introduced isotope carbon atoms. Moreover, TEM observations reveal that the nanotubes are composed of graphitic shells parallel to the tube axis and that the numbers of shells are constant throughout the lengths of the nanotubes. Two conclusions can be drawn from these results. First, all the graphitic shells of the nanotube extrude from the catalyst particle; no direct deposition occurs on the grown tube stem. The absent of such over-coating is desired in terms of synthesizing clean nanotubes for device applications. Second, no separate graphitic shell extrudes over other shells either in the outside or inside of the nanotube. Therefore, we can conclude that synchronized extrusion occurs for all the shells of the multiwalled nanotubes from the catalyst, as suggested in the "Yarmulke" mechianism.[24]

The results in this communication provide a clear picture of the growth process of multiwalled carbon nanotubes in CVD and represent a step forward toward fully understanding the growth mechanism of nanotubes. The method can be naturally extended to study the growth mechanism of single-walled carbon nanotubes. Further, the formation of $^{12}C-^{13}C$ nanotube junctions suggests that nanotube-based intermolecular devices can be obtained by using controlled chemical growth methods. The isotope-labeling method shall also prove powerful in investigating the catalytic growth mechanism of other forms of nanotubes and nanowires.

**Acknowledgment.** We thank M. L. de la Chapelle for valuable discussions on Raman spectroscopy; K. L. Jiang for help in CVD experiment; and D. P. Yu and S. Miao for technical help in electron microscope. This work is supported by the Chinese National Foundation of Natural Science Research and the State Key Project of Fundamental Research of China.

**Supporting Information Available:** Raman modes of pure $^{12}C$ and pure $^{13}C$ multiwalled nanotube arrays and their ratios (PDF). This material is available free of charge via the Internet at http://pubs.acs.org.

JA0167304

(20) Eklund, P. C.; Holden, J. M.; Jishi, R. A. *Carbon* **1995**, *33*, 959.
(21) Rao, A. M.; Jorio, A.; Pimenta, M. A.; Dantas, M. S. S.; Saito, R.; Dresselhaus, G.; Dresselhaus, M. S. *Phys. Rev. Lett.* **2000**, *84*, 1820.
(22) Since the nanotube growth rate tends to decrease with time, we set the growth time under the second isotope ethylene longer than that under the first isotope ethylene in order to obtain half $^{12}C$ segment−half $^{13}C$ segment nanotubes.
(23) The small difference between the Raman spectra at the array bottom and the pure $^{13}C$ spectrum in Figure 2b is attributed to the existence of some residual $^{12}C$ ethylene, which led to some $^{12}C$ atoms in the $^{13}C$ nanotube stem. The coexistence of the two isotopes does not fade away entirely during the short growth time. The same phenomena can be seen in Figure 2c.
(24) Dai, H. J.; Rinzler, A. G.; Nikolaev, P.; Thess, A.; Colbert, D. T.; Smalley, R. E. *Chem. Phys. Lett.* **1996**, *260*, 471.